

## Excitation of Coherent Phonons in Crystalline Bi: Theory for Driving Atomic Vibrations by Femtosecond Pulses

Davide Boschetto<sup>1</sup>, Eugene G. Gamaly<sup>2</sup>, Andrei V. Rode<sup>2</sup>, Thomas Garl<sup>1</sup>, and Antoine Rousse<sup>1</sup>

<sup>1</sup>Laboratoire d'Optique Appliquée, ENSTA, Chemin de la Hunière, Palaiseau, 91761, France

<sup>2</sup>Laser Physics Centre, Research School of Physical Sciences and Engineering, The Australian National University, Canberra, ACT 0200, Australia

### ABSTRACT

In this paper we present experimental and theoretical studies of reflectivity oscillations of an optical probe beam reflected from a single-crystal of bismuth excited by 35 fs laser pulses at deposited energy density above the melting temperature. Coherent and incoherent lattice dynamics as well as electrons dynamics were investigated starting from the reflectivity changes, measured with high accuracy  $\Delta R/R < 10^{-5}$ . The complex behaviour of the reflectivity could not be explained in the light of the existing theories. Therefore, we developed a new theory, starting from the very basic principles of laser-matter interaction, which shows good agreement with experimental results. We establish a direct dependence of the transient reflectivity on atomic motions driven by electron temperature gradient through electron-phonon coupling.

### INTRODUCTION

Coherent optical phonons has received a lot of attention with the advent of femtosecond lasers, as the pump-probe technique provides a means to follow the lattice dynamics after the excitation with sub-picosecond resolution. Optical phonons can be seen as an elementary atomic movement, and therefore their knowledge is a key point to understand the structural dynamics. In particular, exciting a selected phonon mode will pave the way to control phase transitions. Possible applications are phase transitions like the insulator-to-metal transitions, transitions to superconductivity, and many others.

Since the early 1980s a number of experiments have been performed which measured the transient reflectivity and transmission of solids using pump-probe techniques with time resolution around 100 fs [1-13]. The reflectivity of a probe beam as a function of delay following the pump pulse has been measured for a variety of materials, both opaque and transparent, including insulators, semimetals, and semiconductors.

The most salient feature of those measurements was reflectivity oscillations at frequencies corresponding to the optical phonon modes of the material. A number of mechanisms have been proposed to explain those oscillations, including the most frequently cited displacive excitation of coherent phonons (DECP) [2] and impulsive stimulated Raman scattering (ISRS) [3,4]. However, a general theory explaining excitation of atomic vibrations in transparent and opaque media and their connection to reflectivity oscillations is still absent, to the best of our knowledge.

We show that the mechanism of coherent phonon excitation is related to the interplay of several types of forces, which are expressed through the “field+matter” stress tensor. Those forces are related to the polarisation and to the electrons and lattice temperature gradient. On the other hand, the changes in reflectivity are calculated by the changes in the real and imaginary part of the dielectric constant, which depends on electrons density and electron-phonon coupling rate. The last effect is responsible of the observed “oscillations” in reflectivity, as we will show in the following.

## EXPERIMENT

The experiment was carried out in a standard pump-probe geometry by a laser system that could deliver 35 fs pulses at 1 kHz repetition rate, 800 nm wavelength and energy up to 10 mJ. We used an acousto-optical programmable dispersive filter (DAZZLER<sup>TM</sup>) system in order to ensure the pulse was transform-limited at the sample surface in order to achieve high temporal resolution. The pump pulse was chopped at 500 Hz and the probe reflectivity measured using a digital lock-in amplifier. Two features of the experiment allowed us to improve the signal-to-noise ratio. First, we used a phase-locked system where we could modify and control in real-time both the rotation speed and phase of the optical chopper to ensure perfect synchronisation between the chopper and the laser pulse. This avoided any loss of synchronisation due to the mechanical inertia of the optical chopper. Secondly, we adjusted the time-constant of the photodiode response to slightly less than 1 ms (the time between two pulses), to achieve high resolution in the detection of the spectral component at 500 Hz. Our signal-to-noise ratio was as good as  $10^5$  using an integration time of only 1 second. This allowed us to observe reflectivity changes  $\Delta R$  with the accuracy  $\Delta R/R \sim 5 \times 10^{-6}$ . The temporal resolution was determined by the probe pulse duration and was  $\sim 35$  fs.

The sample was a single crystal of bismuth (111)-oriented with one-side polished to reduce light scattering at the surface. The pump and probe pulses were polarised orthogonally to each other to reduce the disturbance of the pump beam into the photodiode used for probe measurement, and focussed to a beam 100  $\mu\text{m}$  in diameter on the sample. The initial reflectivity of the crystal surface was determined by ellipsometry and found to be  $R = 0.74$  at 800 nm at room temperature [17].

Figure 1 shows the time-dependent reflectivity for two pump fluencies: 2.7  $\text{mJ}/\text{cm}^2$  and 6.7  $\text{mJ}/\text{cm}^2$ . These traces contain characteristic features that were observed at all pump fluencies in the range 1.5  $\text{mJ}/\text{cm}^2$  to 15  $\text{mJ}/\text{cm}^2$ . For an instant the reflectivity drops below the unperturbed value before increasing above the initial level reaching a maximum about 300 fs after the excitation pulse. The reflectivity then oscillates with a fluence-dependent frequency and with amplitude, which decays nearly exponentially with time. About 10 ps after the excitation pulse the signal again drops below the unperturbed level and remains constant and below this level for  $\sim 20$  ps, before slowly returning to the unperturbed value  $\sim 4$  ns after excitation. This indicated that material excitation was fully reversible. The frequency of the reflectivity oscillations for pump fluence 2.7  $\text{mJ}/\text{cm}^2$  coincided with the value of the  $A_{1g}$  optical mode of bismuth at 2.9 THz. The frequency decreased with increasing pump fluence (at 6.7  $\text{mJ}/\text{cm}^2$  it was 2.86 THz) in agreement with previous experiments [2,4-6]. A novel feature observed in these experiments, was the presence of the initial sharp drop of the reflectivity, which we could only observe when the time resolution was better than 40 fs.

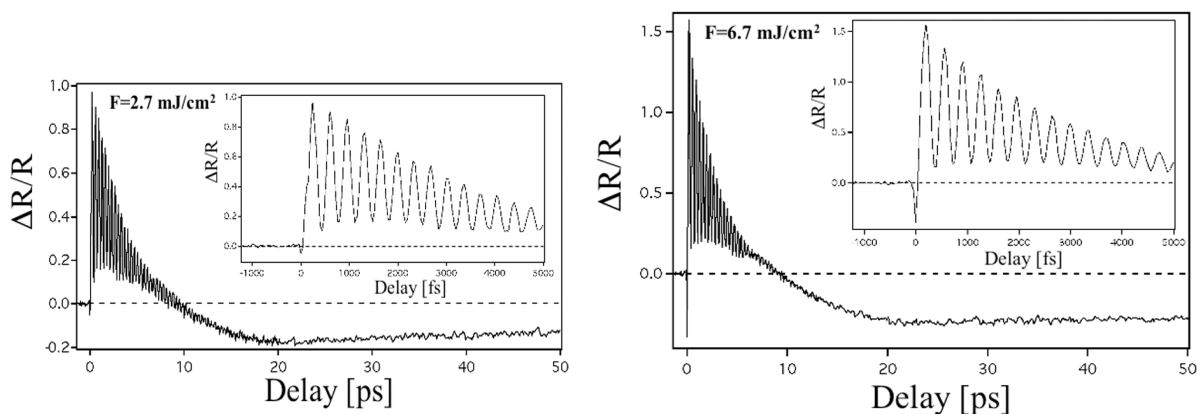


**Figure 1:** Reflectivity changes in bismuth as function of the pump-probe delay, for excitation flux 2.7  $\text{mJ}/\text{cm}^2$  and 6.7  $\text{mJ}/\text{cm}^2$ .

## THEORY

In order to study the behaviour of the reflectivity, two main points must be considered. First, we consider the mechanisms of phonons excitation by the forces imposed on the crystal by the pump pulse. Second, we describe how reflectivity changes due to the phonons excitation. We analyse them in succession starting from the arrival of the laser pulse.

Atomic displacement during the pulse occurs due to a rapid shift [2] in the atomic position by forces,  $f$ , exerted by the laser. These forces are expressed through the “field + matter” stress tensor  $\sigma_{ik}$ , as the following [18]:

$$f_i = \frac{\partial \sigma_{ik}}{\partial x_k} = \frac{\partial P}{\partial x_i} + \frac{\partial(\Delta\varepsilon)_{lk}}{\partial x_i} \frac{E_l E_k}{8\pi} + \frac{(\Delta\varepsilon)_{lk}}{8\pi} \frac{\partial(E_l E_k)}{\partial x_i} = f_{therm} + f_{pol} + f_{pond} \quad (1)$$

where  $P$  is electron and lattice pressure. The total force is a sum of the thermal force  $f_{th}$ , acting along the normal to the surface, z-direction), which is proportional to the electron and lattice pressure gradients; the polarisation force  $f_{pol}$ , acting along the surface, where x-direction is the direction of the linearly polarised pump pulse, which is proportional to laser intensity (the impulsive Raman effect [3,14]); and the ponderomotive force  $f_{pond}$ , that can be neglected here. The amplitude  $q$  of atomic shift under action of above forces during pulse time,  $t_p$ , expresses as:  $q_{x,z} \approx f_{th,pol} \cdot t_p^2 / \rho$  ( $\rho$  is the mass density). The change of dielectric function due to both forces is proportional to atomic shift in accord with the Placzek model [14]  $(\Delta\varepsilon)_{r,p} \approx 4\pi\chi_0(\Delta q_x + \Delta q_z) / d_0 \sim 10^{-4} - 10^{-5}$  ( $\chi_0 \sim 0.2$  is zero order polarizability; and  $d_0 \sim 4 \times 10^{-8}$  cm is inter-atomic distance). Thus, the polarisation-related change in reflectivity during the pulse is negative  $\Delta R_{pol} \sim \{-10^{-4}, -10^{-5}\}$  and proportional to the laser intensity,  $\Delta R_{pol} = -C_1 \cdot I$ , which is in qualitative agreement with the experiments.

The absorbed laser energy produces transition of electrons from valence to conduction band, which is proportional to the electrons temperature. Evolution of electrons and lattice temperatures is described by the well-known two-temperatures model.

The total thermal force includes components due to both the (decreasing) electronic temperature and (increasing) lattice temperature and acts in the z-direction displacing the atoms,  $f_{th} = [T_e(t) + T_L(t)] / l_s$ . One can describe the vibrations up to the melting point as an approximate solution of equation for damped harmonic oscillations in accordance to [3,14]:

$$\Delta q(t) \approx \{f_{th}(t) / m_a \omega_0 \gamma\} \cdot e^{-\gamma t} \cos\left\{(\omega_0^2 - \gamma^2)^{1/2} t + \varphi\right\} \quad (2)$$

where  $m_a$  is the atomic mass,  $\omega_0$  is the phonon frequency, and  $\gamma$  and  $\varphi$  are the phenomenological damping and phase shift respectively. Thus all parameters in laser-excited solid are functions of time-dependent electron  $T_e(t)$ , and lattice,  $T_L(t)$ , temperature. These temperatures have been calculated from coupled electron and lattice energy equations in two-temperature approximation [23] and the material data from [15-17]. The maximum electron temperatures at the end of the pulse were calculated using energy conservation assuming that all the absorbed laser energy at the end of the pulse is in the electron component. It was calculated to be  $T_{e,m} = 3,100$  K at  $2.7$  mJ/cm<sup>2</sup> and  $4,700$  K at  $6.7$  mJ/cm<sup>2</sup>, while the lattice temperature after the electron-lattice equilibration reached in  $\sim 20$  ps was, correspondingly,  $701.5$  K and  $1,273$  K. Therefore Bi could be transformed into disordered state after temperature equilibration with only one symmetry independent optical mode.

the reflectivity variations of a probe can be expressed through the changes in the dielectric function, which in turn are explicit functions of time-dependent electron and lattice temperatures. Indeed:

$$\Delta R = \left( \frac{\partial R}{\partial \varepsilon_r} \right) \Delta \varepsilon_{pol} + \left( \frac{\partial R}{\partial \varepsilon_r} \right) \Delta \varepsilon_{e,r} + \left( \frac{\partial R}{\partial \varepsilon_i} \right) \Delta \varepsilon_{e,i} . \quad (3)$$

The coefficients in (3) are determined from the unperturbed values of the dielectric function for Bi at 800 nm,  $\varepsilon_r = -16.25$ ,  $\varepsilon_i = 15.4$ ;  $R = 0.74$  [15-17] with the help of the Fresnel formula [18]. It follows that for Bi at 800 nm,  $\frac{\partial R}{\partial \varepsilon_r} < 0$ ;  $\frac{\partial R}{\partial \varepsilon_i} > 0$ , which is typical for good metals.

The real part of the dielectric function for semi-metals can be considered as the sum of a positive atomic (ionic) term and negative electronic term along with the electronic imaginary part, responsible for absorption. The changes in dielectric function are due to the changes in polarisation, free electrons density and electrons phonon collision frequency

Electronic parts obey the Drude form according to the optical data [14,17-20]:

$$\varepsilon_{el} = \varepsilon'_{el} + i\varepsilon''_{el} = 1 - \frac{\omega_p^2}{\omega^2 + \nu_{e-ph}^2} + i \frac{\omega_p^2}{\omega^2 + \nu_{e-ph}^2} \frac{\nu_{e-ph}}{\omega} \quad (4)$$

Here  $n_e$ ,  $m_e$ ,  $\omega$  are respectively the electron number density, electron mass, and laser frequency;  $\nu_{e-ph}$ , is the electron-phonon momentum exchange rate,  $\omega_p^2 = \frac{4\pi e^2 n_e(t)}{m_e^*}$  is the electron plasma

frequency. It is reasonable to assume that the electron's mass attains its free electron value following the excitation. Therefore, the perturbation in the electronic dielectric function depends on two parameters: electron number density and electron-phonon momentum exchange rate,

$\Delta \varepsilon_{el} = \left( \frac{\partial \varepsilon_{el}}{\partial n_e} \right)_0 \Delta n_e + \left( \frac{\partial \varepsilon_{el}}{\partial \nu_{e-ph}} \right)_0 \Delta \nu_{e-ph}$ . Finally the transient reflectivity in (3) is expressed through the time-dependent electron and lattice temperatures as follows:

$$\Delta R = -C_1 \cdot \Delta \varepsilon'_{pol} + C_2 \cdot \Delta n_e / n_{e,0} - C_3 \cdot \Delta \nu_{e-ph} / \nu_{e-ph} \quad (5)$$

Here  $C_1 = \left( \frac{\partial R}{\partial \varepsilon'} \right)_0$ ;  $C_2$ ,  $C_3$  are expressed through the unperturbed value of the dielectric function.

For Bi  $C_2$  is always positive. Second term in (5) grows up to the end of the laser pulse as the number of excited electrons increases, and after the pulse end it decreases due to recombination.  $C_3$  might be all the time negative depending on the relation of the laser frequency to electron-phonon momentum exchange rate that is responsible for absorption.

The perturbation in the electron-phonon coupling rate under laser excitation readily expresses through variation in lattice temperature and phonon's amplitude [21,22]:

$$\Delta \nu_{e-ph} / \nu_{e-ph}^{(0)} = \Delta T_L / T_0 + 2\Delta q(t) / q_0; \quad (6)$$

here zero denotes initial room temperature and phonon's amplitude. Maximum electron temperature is much smaller than the Fermi energy that can be extracted from the optical measurements [14,17,18]. Therefore one can neglect velocity changes due to temperature in comparison to the Fermi velocity,  $v_e \ll v_F$ . Substituting (6) into (5) one expresses the reflectivity changes under laser excitation through perturbation in polarisation, number density of excited electrons, lattice temperature and atomic motion.

$$\Delta R = -C_1 \Delta \varepsilon'_{pol} + C_2 \Delta n_e / n_{e,0} - C_3 \Delta T_L / T_0 - C_4 \Delta q(t) / q_0 \quad (7)$$

The signs of normalisation coefficients,  $C_i$ , are defined by the unperturbed optical properties of Bi crystal [24];  $\Delta q(t)$  is defined by (2). The first term in (7) is responsible for the polarisation during the pulse. The second term emphasises the increase in reflectivity due electron excitation from the valence to the conduction band. The 3<sup>rd</sup> and 4<sup>th</sup> terms come from the electron-phonon coupling that is responsible for the lattice heating and this gradually reduces the reflectivity after the pulse.

It follows from (7) that during the pulse the first two terms with the effects of opposite sign compete. The polarisation component switches on from the very beginning while the number of free carriers, that is proportional to the electron temperature, grows up during the pulse. Therefore the first negative initial drop in reflectivity should be always present early in the pulse until the second term in (7) becomes dominant. The amplitude of the initial drop is proportional to the laser intensity in agreement with the experiments. The reflectivity reaches its maximum after approximately one phonon period due to electron excitation and heating. Afterwards phonons oscillations become apparent in the time-dependence of the reflectivity.

The calculated  $\Delta R/R$  function is presented at Fig. 2, and compared with the experimental data. There are several distinguishable features in the reflectivity behaviour. First, the sharp initial drop in reflectivity was observed experimentally with 35 fs pump-probe, while with lower temporal resolution of 50 fs it was not detected that qualitatively agrees with the theory. Second, after reaching maximum, the reflectivity starts oscillating with the period corresponding to the  $A_{1g}$  phonon frequency, 2.9 THz at laser fluence  $2.7 \text{ mJ/cm}^2$ , and 2.86 THz at  $6.7 \text{ mJ/cm}^2$  that is the mode softening observed before [4-6]. The damping of the oscillations, with  $\gamma = 3.4 \times 10^{11} \text{ s}^{-1}$  results from multi-phonon processes (anharmonicity) that finally terminates harmonic vibrations due to lattice temperature increase up to the melting point. Note, that duration of the period where harmonic oscillations are discernible decreases with the increase in the pump fluence in qualitative agreement with the above considerations. Thirdly, the average value of the oscillating reflectivity drops below the unperturbed level after approximately 10 ps due to free carrier recombination and electron to-lattice temperature equilibration.

Theoretical prediction based on Eq.(7) fits well to experiments during the first 25 ps. Slight discrepancy for longer period most probably relates to the heat diffusion from the skin layer, which was not included into calculations. A deeper insight into the optical changes of photo-excited bismuth as well as a further proof of the validity of our model could be obtained by measuring the transient real and imaginary part of the dielectric constant, as suggested by [25]. In this case, one could measure directly the time-dependent electron-phonon collision rate as well as the change in plasma frequency [26].

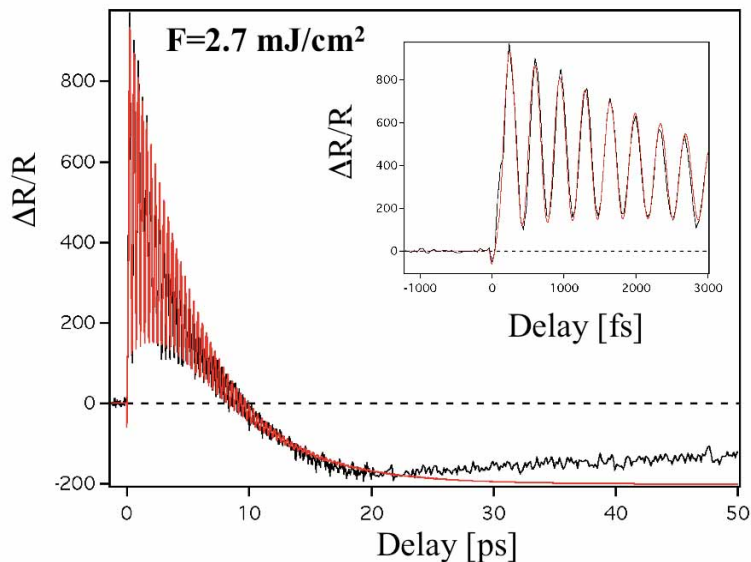


**Figure 2:** Comparison between the experimental and theoretical behaviour of the reflectivity at  $2.7 \text{ mJ/cm}^2$  laser excitation flux.

## CONCLUSIONS

In conclusion, we presented new experimental results of pump-probe reflectivity measurements from bismuth single crystal with high sensitivity and time resolution. The existing models could not explain the complex behaviour of the reflectivity. Therefore, we propose a new theory, by which the behaviour of reflectivity can be recovered without ad-hoc assumption. We show that reflectivity oscillations are related to the atomic vibrations via the electron-phonon coupling and due to change in polarisation.

We demonstrated that thermal and polarisation forces are driving atomic vibrations of different symmetry at different intensities, in transparent and opaque media. Therefore, one can expect simultaneous excitation of  $A_{1g}$  and  $E_{1g}$  modes by a single pulse with appropriate polarisation and intensity. Amplitude's ratio for two modes then shall be proportional to the ratio of forces in [111] direction and (111) plane, respectively. This opens a route for controlled excitation of phonons of arbitrary symmetry.

## ACKNOWLEDGEMENTS

EGG, and AVR gratefully acknowledge the useful discussions with Prof. B. Luther-Davies and the support of the Australian Research Council through its Discovery program. The support of Programme International De Cooperation Scientifique (PICS, France) is gratefully acknowledged.

## References

1. A. Rousse *et al.*, Nature **410**, 65, (2001).
2. H. J. Zeiger *et al.*, Phys. Rev. B **45**, 768 (1992).
3. R. Merlin, Solid State Comm. **102**, 207 (1997).
4. G. A. Garret *et al.*, Phys. Rev. Letters **77**, 3661 (1996).
5. M. Hase *et al.*, Appl. Phys. Letters **69**, 2474 (1996).
6. E. D. Murray *et al.*, Phys. Rev. B **72**, 060301(R) (2005), and references herein.
7. K. Ishioka *et al.*, Journ. of Appl. Phys. **100**, 093501 (2006).
8. K. Sokolowski-Tinten *et al.*, Nature **422**, 287 (2003).
9. A. Cavalleri *et al.*, Phys. Rev. Letters **87**, 237401 (2001).
10. E. Collet *et al.*, Science **300**, 612 (2003).
11. T. Dumitrica *et al.* Phys. Rev. Letters **92**, 117401 (2004).
12. M. Chollet *et al.*, Science **307**, 86 (2005).
13. A.J. Kent *et al.*, Phys. Rev. Letters **96**, 215504 (2006).
14. T. Garl, Ellipsometry of Bismuth at room temperature (unpublished, 2006).
15. L.D. Landau, E.M. Lifshitz, L. P. Pitaevskii, *Electrodynamics of Continuous Media*, (Pergamon Press, Oxford, 1984).
16. Y.R. Shen & N. Bloembergen, Phys. Rev. **137**, 1787 (1965).
17. M. I. Kaganov, *et al.*, Sov. Phys. JETP **4**, 173 (1957).
18. *American Institute of Physics Handbook*, D.E. Gray, Ed., 3d edition, (McGraw-Hill Book Company, New York, 1972).
19. Landolt-Bornstein, *Numerical Data and Functional relationships in Science and Technology, Group III, vol 17, Semiconductors* (Springer-Verlag, Berlin, 1983).
20. Real and imaginary parts of the Drude dielectric function are [18]:  $\epsilon_r = 1 - \omega_p^2 / (\omega^2 + \nu_{e-ph}^2)$ ,  $\epsilon_i = (1 - \epsilon_r) \nu_{e-ph} / \omega$ . Then,  $\Delta \epsilon_{r,i} = (\partial \epsilon_{r,i} / \partial n_e) \Delta n_e + (\partial \epsilon_{r,i} / \partial \nu_{e-ph}) \Delta \nu_{e-ph}$ . The coefficients (derivatives) are calculated using the optical data from [15-17].
21. A. A. Abrikosov, Sov. Phys. JETP **17**, 1372 (1963).

22. M. Ziman, “*Electrons and Phonons*”, (Clarendon Press, Oxford, 1960).

23. Electron-phonon coupling represents the interaction between electron charge,  $e$ , and the dipole electric field of polarized charge created by lattice vibrations,  $E_{ph} \approx eq/d^3$  ( $d$  is interatomic distance). The electron-phonon momentum exchange rate expresses through the energy of interaction,  $\varepsilon_{ph} \approx qeE_{ph} \approx e^2q^2/d^3$  in agreement with the kinetic approach [21]:  
 $v_{e-ph} \approx \varepsilon_{ph}/\hbar \approx n_{ph}q^2v_e$ ;  $v_e \approx e^2/\hbar$  is electron velocity,  $n_{ph} \approx d^{-3}$  is the phonon’s density.

$$24. C_1 \sim A_1 = \left( \frac{\partial R}{\partial \varepsilon_r} \right)_0 < 0; C_2 \sim A_2 = (\varepsilon_{r,m} - 1) \cdot \left( \frac{\partial R}{\partial \varepsilon_{r,m}} \right)_0 + \varepsilon_{i,m} \cdot \frac{\partial R}{\partial \varepsilon_{i,m}} > 0;$$

$$C_3, C_4 \sim A_3 = \frac{2\varepsilon_i \omega \nu}{\omega^2 + \nu^2} \cdot \left( \frac{\partial R}{\partial \varepsilon_{e,r}} \right)_0 + \varepsilon_{e,i} \cdot \frac{(\omega^2 - \nu^2)}{(\omega^2 + \nu^2)} \cdot \left( \frac{\partial R}{\partial \varepsilon_{e,i}} \right)_0 < 0. \text{ Here } \nu - \text{ is electron-phonon}$$

momentum exchange rate,  $\omega$  is the laser frequency.

25. C. A. D. Roeser, *et al.*, Rev. Sci. Instr. **74**, 3413 (2003).

26. O. P. Uteza, *et al.*, Phys Rev B **70**, 054108 (2004).